Advances in Applied Mathematics and Mechanics
Adv. Appl. Math. Mech., Vol. **15**, No. x, pp. 1-22

DOI: 10.4208/aamm.OA-2021-0373
xxx 2023

# Calculation of Four-Dimensional Unsteady Gas Flow via Different Quadrature Schemes and Runge-Kutta 4th Order Method

M. Salah[1], M. S. Matbuly[1], O. Civalek[2,*] and Ola Ragb[1]

[1] *Department of Engineering Mathematics and Physics, Faculty of Engineering, Zagazig University, P.O. 44519, Egypt*
[2] *Akdeniz University, Department of Civil Engineering, Antalya, Turkey*

Received 13 December 2021; Accepted (in revised version) 27 September 2022

**Abstract.** In this study, a $(3+1)$ dimensional unstable gas flow system is applied and solved successfully via differential quadrature techniques based on various shape functions. The governing system of nonlinear four-dimensional unsteady Navier–Stokes equations of gas dynamics is reduced to the system of nonlinear ordinary differential equations using different quadrature techniques. Then, Runge-Kutta 4th order method is employed to solve the resulting system of equations. To obtain the solution of this equation, a MATLAB code is designed. The validity of these techniques is achieved by the comparison with the exact solution where the error reach to $\leq 1\times 10^{-5}$. Also, these solutions are discussed by seven various statistical analysis. Then, a parametric analysis is presented to discuss the effect of adiabatic index parameter on the velocity, pressure, and density profiles. From these computations, it is found that Discrete singular convolution based on Regularized Shannon kernels is a stable, efficient numerical technique and its strength has been appeared in this application. Also, this technique can be able to solve higher dimensional nonlinear problems in various regions of physical and numerical sciences.

**AMS subject classifications**: 34B05, 76N15, 35G15, 65F05, 65F10, 65F45

**Key words**: Statistical analysis, Runge-Kutta, discrete singular convolution, sinc, quadrature approach, gas dynamics, adiabatic index.

## 1 Introduction

Fluid mechanics play a significant role in this work by unsteady gas flow. Unsteady gas flow of an ideal polytropic gas in three-dimensional is a system of nonlinear partial differential equation. The dynamic flow of incompressible fluid is defined via Navier–Stokes

*Corresponding author.
*Email:* civalek@yahoo.com (O. Civalek)

 

(N-S) equations where the unknowns are the velocity, pressure, and density as functions of space $(x,y,z)$ and time variables [1,2]. A result of these equations forecasts the manner of the fluid, assuming its initial and boundary conditions are known. So, these equations are considered one of the extreme important types of mathematical physics [3-5].

Recently, researchers applied different methods to get the exact and numerical results of these problems. Raja et al. [6,7] applied the Lie group of transformations technique to get the result of unsteady Euler system of gas dynamics. Also, Rashed [8] solved the previous system via an optimal equation of Lie symmetry vectors. Asymmetry analysis was applied by Fuchs and Richter [9]. Lie symmetries was developed by Murata [10] to obtain the solution of 2-D system in radial coordinates. Further, Arora et al. [11] investigated strong shocks in a non-perfect relaxing gas by the previous technique. Substitution principles were carried out by Oliveri and Speciale [12-18] to solve the unsteady equations of ideal gases and perfect magneto-gas dynamics equations. Chirkunov et al. [19] analyzed the gas dynamics with zero sound velocity. There are a lot of numerical techniques to solve N-S equations where these systems are nonlinear and complicated. Babaev et al. [20] demonstrated solution for Navier–Stokes system via Variational Iterative techniques. Numerous contributions in analysis Navier–Stokes system using Finite difference (FD) scheme have been published by various authors [21-23]. Zhao et al. [24] studied the original boundary condition-enforced immersed boundary method for simulation of incompressible flows having moving boundaries. Yuan et al. [25] examined a new gas-kinetic flux solver to simulate the compressible and incompressible flows for continuum and slip regimes by using finite volume method and Boltzmann equation. Many software programs are developed depending on Implicit Finite Difference schemes like MIKE-11 [26] and HEC-RAS [27] for solving the nonlinearity of unsteady flow equations. Zhou et al. [28] implemented the circular function-based gas-kinetic scheme to moving boundary problems for moving grids with finite volume method. A simplified and efficient multiphase lattice Boltzmann flux solver model was proposed for multiphase flows large density ratio by Yang et al. [29] The extrapolation formulation was presented to compute the compressible Navier–Stokes–Fourier equations that considers slip and jump boundary conditions by Shterev [30]. Lai [31] used method of characteristics (MOC) for solving the unsteady open-channel flow. This method depends on the choice of grid points to achieve stability, it is also complex and needs more time in programming compared to the other schemes. But the researchers investigated and developed a new numerical scheme with more convergence, stable and efficiency to raise numerical modeling abilities. Differential quadrature (DQ) scheme has been developed to solve different differential equations as linear or nonlinear. Differential quadrature (DQ) technique is a stable, converge, and efficient technique for solving various problems of fluid mechanics with small number of points and less calculations effort [32-37,40]. Shu [32,37] issued different searches for solving N–S equations and boundary condition in the field of fluid mechanics by generalized differential quadrature method (GDQM). Rosa et al [38] applied Differential quadrature technique to estimate the identification of the stiffness of structural elements. Alqahtani and Jiwari [39] studied the features of nanofluid flow and thermal transmission (NFTT) in a rectangular channel which is asymmetric by developing two numerical algorithms based on scale-2 Haar wavelets (S2HWs), Lagrange's interpolation differential quadrature technique (LIDQT), and quasi linearization process (QP). Mohammad et al. [40] employed DQM for numerical simulation of unsteady open channel flow. The articles published via DQM solving the steady-state of N-S equations are limited. To overcome time dependent problems, DQM can be combined with Runge Kutta, block marching, and finite difference techniques to discretize the time domain [41-44]. Salah et al. [45-47] solved nonlinear partial differential equations by classical DQM with Explicit and Implicit Euler method, Runge–Kutta 4th order (RK4), and Block marching to overcome time dependent problems.

RK4 technique is a numerically scheme mostly applied to solve Initial Value equations, due to its speed and accuracy requiring less computation of higher-order derivative [45-47]. Birken [41] employed Runge-Kutta smoothers to get the solution of unsteady viscous flow problems. Jameson [42] presented an estimate of totally implicit Runge-Kutta techniques for solving unsteady flow computations. Sheng [43] used Runge-Kutta techniques with compact Difference methods for solving the unsteady Euler equations. Tamsir et al. [48-56] solved various nonlinear partial differential equations using modified cubic B-spline DQM (MCB-DQM), in space to transform the system of partial differential equations (PDE) to system of ordinary differential equations (ODE). The solution is completed by employing a five stage and fourth-order strong stability preserving Runge–Kutta algorithm, in time (SSP-RK54).

Here, optimal schemes of differential quadrature are developed for applying in mathematical analysis of $(3+1)$-dimensional unsteady turbulent gas flow equations which defined from the general N–S equations. Different schemes of DQM depend on shape function like the Polynomial Differential quadrature (PDQ) technique, Sinc Differential quadrature (SDQ) [55-59] and Discrete Singular convolution (DSC) based on Delta Lagrange (DLK) and Regularized Shannon kernels (RSK) [60-69]. These methods of DQ reduce the system of unsteady gas flow into nonlinear system of ordinary differential equations. After that, the acquired system is computed by RK4. For each scheme, a MATLAB code is designed. Also, the stability, convergence, and efficiency of the presented techniques are determined. The computed solutions are discussed by various statistical analysis such as the rate of convergence, order of convergence, absolute error, RMS, $L_2$ and $L_\infty$ errors [70,71]. Moreover, a parametric study is discussed to show the effect of adiabatic index on the velocity, pressure, and density components.

## 2 Model formulation of the problem

The governing equations for unsteady flow of ideal polytropic gas in $(3+1)$-dimensional can be described as [6-8]:

$$\frac{\partial\rho}{\partial t}+\rho\Big(\frac{\partial u}{\partial x}+\frac{\partial v}{\partial y}+\frac{\partial w}{\partial z}\Big)+u\frac{\partial\rho}{\partial x}+v\frac{\partial\rho}{\partial y}+w\frac{\partial\rho}{\partial z}=0, \tag{2.1a}$$

$$\frac{\partial u}{\partial t}+u\frac{\partial u}{\partial x}+v\frac{\partial u}{\partial y}+w\frac{\partial u}{\partial z}+\frac{1}{\rho}\frac{\partial p}{\partial x}=0, \tag{2.1b}$$

$$\frac{\partial v}{\partial t}+u\frac{\partial v}{\partial x}+v\frac{\partial v}{\partial y}+w\frac{\partial v}{\partial z}+\frac{1}{\rho}\frac{\partial p}{\partial y}=0, \tag{2.1c}$$

$$\frac{\partial w}{\partial t}+u\frac{\partial w}{\partial x}+v\frac{\partial w}{\partial y}+w\frac{\partial w}{\partial z}+\frac{1}{\rho}\frac{\partial p}{\partial z}=0, \tag{2.1d}$$

$$\frac{\partial p}{\partial t}+\gamma p\Big(\frac{\partial u}{\partial x}+\frac{\partial v}{\partial y}+\frac{\partial w}{\partial z}\Big)+u\frac{\partial p}{\partial x}+v\frac{\partial p}{\partial y}+w\frac{\partial p}{\partial z}=0, \tag{2.1e}$$

$$0\le t\le T,\quad X_1\le x\le X_2,\quad Y_1\le y\le Y_2,\quad Z_1\le z\le Z_2, \tag{2.1f}$$

where $x$, $y$, and $z$ are the space coordinates, $t$ is the time, $u$, $v$, and $w$ are the velocity components. $\rho$ and $p$ are the density and pressure, respectively. $\gamma$ is the adiabatic index $(\gamma>1)$.

Boundary conditions are determined as:

At $(x_1,y,z,t)$:

$$A_1u+B_1\frac{\partial u}{\partial x}=F_1(y,z,t),\quad A_3v+B_3\frac{\partial v}{\partial x}=F_3(y,z,t),\quad A_5w+B_5\frac{\partial w}{\partial x}=F_5(y,z,t), \tag{2.2a}$$

$$A_7p+B_7\frac{\partial p}{\partial x}=F_7(y,z,t),\quad A_9\rho+B_9\frac{\partial \rho}{\partial x}=F_9(y,z,t). \tag{2.2b}$$

At $(x_2,y,z,t)$:

$$A_2u+B_2\frac{\partial u}{\partial x}=F_2(y,z,t),\quad A_4v+B_4\frac{\partial v}{\partial x}=F_4(y,z,t),\quad A_6w+B_6\frac{\partial w}{\partial x}=F_6(y,z,t), \tag{2.3a}$$

$$A_8p+B_8\frac{\partial p}{\partial x}=F_8(y,z,t),\quad A_{10}\rho+B_{10}\frac{\partial \rho}{\partial x}=F_{10}(y,z,t). \tag{2.3b}$$

At $(x,y_1,z,t)$:

$$A_{11}u+B_{11}\frac{\partial u}{\partial y}=F_{11}(x,z,t),\quad A_{13}v+B_{13}\frac{\partial v}{\partial y}=F_{13}(x,z,t),\quad A_{15}w+B_{15}\frac{\partial w}{\partial y}=F_{15}(x,z,t), \tag{2.4a}$$

$$A_{17}p+B_{17}\frac{\partial p}{\partial y}=F_{17}(x,z,t),\quad A_{19}\rho+B_{19}\frac{\partial \rho}{\partial y}=F_{19}(x,z,t). \tag{2.4b}$$

At $(x,y_2,z,t)$:

$$A_{12}u+B_{12}\frac{\partial u}{\partial y}=F_{12}(x,z,t),\quad A_{14}v+B_{14}\frac{\partial v}{\partial y}=F_{14}(x,z,t),\quad A_{16}w+B_{16}\frac{\partial w}{\partial y}=F_{16}(x,z,t), \tag{2.5a}$$

$$A_{18}p+B_{18}\frac{\partial p}{\partial y}=F_{18}(x,z,t),\quad A_{20}\rho+B_{20}\frac{\partial \rho}{\partial y}=F_{20}(x,z,t). \tag{2.5b}$$

At $(x,y,z_1,t)$:

$$A_{21}u+B_{21}\frac{\partial u}{\partial z}=F_{21}(x,y,t),\quad A_{23}v+B_{23}\frac{\partial v}{\partial z}=F_{13}(x,y,t),\quad A_{25}w+B_{25}\frac{\partial w}{\partial z}=F_{15}(x,y,t), \tag{2.6a}$$

$$A_{27}p+B_{27}\frac{\partial p}{\partial z}=F_{17}(x,y,t),\quad A_{29}\rho+B_{29}\frac{\partial \rho}{\partial z}=F_{19}(x,y,t). \tag{2.6b}$$

At $(x,y,z_2,t)$:

$$A_{22}u+B_{22}\frac{\partial u}{\partial z}=F_{22}(x,y,t),\quad A_{24}v+B_{24}\frac{\partial v}{\partial z}=F_{14}(x,y,t),\quad A_{26}w+B_{26}\frac{\partial w}{\partial z}=F_{16}(x,y,t), \tag{2.7a}$$

$$A_{28}p+B_{28}\frac{\partial p}{\partial z}=F_{18}(x,y,t),\quad A_{30}\rho+B_{30}\frac{\partial \rho}{\partial z}=F_{20}(x,y,t). \tag{2.7b}$$

Initial condition is explained as:

$$u(x,y,z,0)=\Phi_1(x,y,z),\quad v(x,y,z,0)=\Phi_2(x,y,z),\quad w(x,y,z,0)=\Phi_1(x,y,z), \tag{2.8a}$$

$$p(x,y,z,0)=\Phi_3(x,y,z),\quad \rho(x,y,z,0)=\Phi_4(x,y,z), \tag{2.8b}$$

where $A_h$, $B_h$, $F_h$, $(h=1,2,\cdots,30)$, and $\Phi_j(x,y)$, $(j=1,\cdots,5)$ are known functions.

# 3 Method of solution

In this section, Lagrange interpolation polynomials, Cardinal sine, delta Lagrange and Regularized Shannon kernels are used as different shape functions. These shape functions are applied as basis for differential quadrature technique. Thus, there are four schemes depend on differential quadrature techniques combined with RK4 and they are employed for solving unsteady turbulent gas flow. RK4 is used to overcome time dependent problems.

Differential quadrature method is realized as the unknown function at any grid spacing $f$ and its derivatives are approximated as a weighted sum of full the functional values at certain grids in all calculation domain as follows [32-47]:

$$f_x(x_i,y_j,z_k,t)=\sum_{r=1}^{N_x}A_{ir}^{(x)}f(x_r,y_j,z_k,t),\quad f_{xx}(x_i,y_j,z_k,t)=\sum_{r=1}^{N_x}B_{ir}^{(x)}f(x_r,y_j,z_k,t), \tag{3.1}$$

where $A^x_{ir}$ and $B^x_{ir}$ are the 1st and 2nd weighting coefficients [32-47].

The computed 1st and 2nd derivatives weighting coefficients are various based on choice of shape function. Thus, here is how to get it [32-47]:

## 3.1 Polynomial Differential Quadrature Method (PDQM)

Firstly, Chebyshev-Gauss-Lobatto nodal points are used to obtain the stable solution as follows [35]:

$$X_r=a+\frac{b-a}{2}\left[1-\cos\frac{(r-1)\pi}{N_x-1}\right],\quad r=1,2,\cdots,N_x,\quad a\le X\le b, \tag{3.2}$$

where $N_x$ represents the number of nodal points.

After using Lagrange interpolation polynomials as base function, the weighting coefficients of 1st and 2nd derivatives, are found as [35]:

$$A_{ir}^{x}=\begin{cases}\dfrac{\prod\limits_{k=1,k\neq i}^{N_x}(X_i-X_k)}{(X_i-X_r)\prod\limits_{k=1,k\neq j}^{N_x}(X_r-X_k)}, & i\neq r,\\ -\sum\limits_{r=1,r\neq i}^{N_x}A_{ir}, & i=r,\end{cases}\qquad B_{ir}^{x}=\begin{cases}2A_{ir}\left(A_{ii}-\dfrac{1}{X_i-X_r}\right), & i\neq r,\\ -\sum\limits_{r=1,r\neq i}^{N_x}B_{ir}, & i=r.\end{cases}\tag{3.3}$$

## 3.2 Sinc Differential Quadrature Method (SDQM)

In this scheme, the stability of results depends on discretize the spatial area via uniform nodal points as follows [57-59]:

$$F(X_i)=\sum_{r=-N_x}^{N_x}\frac{\sin[\pi(X_i-X_r)/m_X]}{\pi(X_i-X_r)/m_X}f(X_r),\quad (i=-N_x,N_x),\quad m_X>0.\tag{3.4}$$

After applying Cardinal sine as base function and differentiating Eq. (3.4), the weighting coefficients $A_{ir}^{x}$, $B_{ir}^{x}$ are given as:

$$A_{ir}^{x}=\begin{cases}\dfrac{(-1)^{i-j}}{m_X(i-j)}, & i\neq r,\\ 0, & i=r,\end{cases}\qquad B_{ir}^{x}=\begin{cases}\dfrac{-2(-1)^{i-r}}{m_X{}^2(i-r)^2}, & i\neq r,\\ \dfrac{-\pi^2}{3m_X{}^2}, & i=r,\end{cases}\tag{3.5}$$

where $m_X$ is grid size.

## 3.3 Discrete Singular Convolution Differential Quadrature Method (DSCDQM)

In this technique, the stability of results based on discretize the spatial area via uniform nodal points and the choice of type kernels. For fluid mechanics, Delta Lagrange Kernel (DLK) and Regularized Shannon kernel (RSK) are used for like problem as follows [60-69]:

1. For DSCDQM-DLK, which used Delta Lagrange Kernel as base function, the value of $A_{ir}^{x}$ and $B_{ir}^{x}$ are found as [60-69]:

$$F(X_i)=\sum_{r=-S}^{S}\frac{\prod\limits_{k=-S}^{S}(X_i-X_k)}{(X_i-X_r)\prod\limits_{r=-S,r\neq k}^{S}(X_r-X_k)}f(X_r),\quad (i=-S,S),\quad S\geq 1,\tag{3.6a}$$

$$A^x_{ir}=\begin{cases} \dfrac{1}{(X_i-X_r)}\prod\limits_{k=-S,k\neq i,r}^{S}\dfrac{(X_i-X_k)}{(X_r-X_k)}, & i\neq r,\\ -\sum\limits_{r=-S,r\neq i}^{-S}A^x_{ir}, & i=r, \end{cases}\qquad B^x_{ir}=\begin{cases} 2(A^x_{ir}.A^x_{ii}-\dfrac{A^x_{ir}}{(X_i-X_r)}), & i\neq r,\\ -\sum\limits_{r=-S,r\neq i}^{S}B^x_{ir}, & i=r. \end{cases} \tag{3.6b}$$

2. For DSCDQM-RSK, we used Regularized Shannon kernel as base function, the value of $A^x_{ir}$ and $B^x_{ir}$ are defined as [60-69]:

$$F(X_i)=\sum_{r=-S}^{S}\left\langle\frac{\sin[\pi(X_i-X_r)/m_X]}{\pi(X_i-X_r)/m_X}e^{-(\frac{(X_i-X_r)^2}{2\xi^2})}\right\rangle f(X_r),\quad (i=-N_x,N_x),\quad \xi=(g*m_X)>0, \tag{3.7a}$$

$$A^x_{ir}=\begin{cases} \dfrac{(-1)^{i-r}}{m_X(i-r)}e^{-m^2{}_X(\frac{(i-r)^2}{2\xi^2})}, & i\neq r,\\ 0, & i=r, \end{cases}\qquad B^x_{ir}=\begin{cases} \Big(\dfrac{2(-1)^{i-r+1}}{m_X{}^2(i-r)^2}+\dfrac{1}{\xi^2}\Big)e^{-m^2_X(\frac{(i-r)^2}{2\xi^2})}, & i\neq r,\\ -\dfrac{1}{\xi^2}-\dfrac{\pi^2}{3m_X{}^2}, & i=r, \end{cases} \tag{3.7b}$$

where $2S+1$ is the effective calculation bandwidth, $\xi$ and $g$ are the regularization and computational parameters, respectively.

The problem is diminished to nonlinear ordinary differential equations by substituting from Eq. (3.1) into Eqs. (2.1a)-(2.1e) as follow:

$$\begin{aligned}\frac{d\rho}{dt}\Big|(x_i,y_j,z_k,t)=&-\rho\Big[\sum_{r=1}^{N_x}A^x_{ir}u(x_r,y_j,z_k,t)+\sum_{l=1}^{N_y}A^y_{jl}v(x_i,y_l,z_kt)\\ &+\sum_{n=1}^{N_z}A^z_{kn}v(x_i,y_l,z_kt)\Big]-u_{ijk}\sum_{r=1}^{N_x}A^x_{ir}\rho(x_r,y_j,z_k,t)\\ &-v_{ijk}\sum_{l=1}^{N_y}A^y_{jl}\rho(x_i,y_l,z_kt)-w_{ijk}\sum_{n=1}^{N_z}A^z_{kn}v(x_i,y_l,z_kt),\end{aligned} \tag{3.8a}$$

$$\begin{aligned}\frac{du}{dt}\Big|(x_i,y_j,z_k,t)=&-u_{ijk}\sum_{r=1}^{N_x}A^x_{ir}u(x_r,y_j,z_k,t)-v_{ijk}\sum_{l=1}^{N_y}A^y_{jl}u(x_i,y_l,z_kt)\\ &-w_{ijk}\sum_{n=1}^{N_z}A^z_{kn}u(x_i,y_l,z_kt)-\frac{1}{\rho_{ijk}}\sum_{r=1}^{N_x}A^x_{ir}p(x_r,y_j,z_k,t),\end{aligned} \tag{3.8b}$$

$$\begin{aligned}\frac{dv}{dt}\Big|(x_i,y_j,z_k,t)=&-u_{ijk}\sum_{r=1}^{N_x}A^x_{ir}v(x_r,y_j,z_k,t)-v_{ijk}\sum_{l=1}^{N_y}A^y_{jl}v(x_i,y_l,z_kt)\\ &-w_{ijk}\sum_{n=1}^{N_z}A^z_{kn}v(x_i,y_l,z_kt)-\frac{1}{\rho_{ijk}}\sum_{l=1}^{N_y}A^y_{jl}p(x_i,y_l,z_kt),\end{aligned} \tag{3.8c}$$

$$\begin{aligned}\frac{dw}{dt}\Big|(x_i,y_j,z_k,t)=&-u_{ijk}\sum_{r=1}^{N_x}A^x_{ir}w(x_r,y_j,z_k,t)-v_{ijk}\sum_{l=1}^{N_y}A^y_{jl}w(x_i,y_l,z_kt)\\ &-w_{ijk}\sum_{n=1}^{N_z}A^y_{kn}w(x_i,y_l,z_kt)-\frac{1}{\rho_{ijk}}\sum_{n=1}^{N_z}A^y_{kn}p(x_i,y_l,z_kt),\end{aligned} \tag{3.8d}$$

$$\begin{aligned}\frac{dp}{dt}\Big|(x_i,y_j,z_k,t)=&-\gamma p_{ijk}\Big[\sum_{r=1}^{N_x}A_{ir}^{x}u(x_r,y_j,z_k,t)+\sum_{l=1}^{N_y}A_{jl}^{y}v(x_i,y_l,z_kt)\\&+\sum_{n=1}^{N_z}A_{kn}^{z}v(x_i,y_l,z_kt)\Big]-u_{ijk}\sum_{r=1}^{N_x}A_{ir}^{x}p(x_r,y_j,z_k,t)\\&-v_{ijk}\sum_{l=1}^{N_y}A_{jl}^{y}p(x_i,y_l,z_kt)-w_{ijk}\sum_{n=1}^{N_z}A_{kn}^{z}p(x_i,y_l,z_kt).\end{aligned}\tag{3.8e}$$

Boundary conditions and initial conditions are augmented in the governing equations. Then, the Runge-Kutta 4th order scheme is applied to solve the nonlinearity ODE's equations [41-47].

### 3.4 Runge-Kutta 4th order (RK4) method

To overcome the transient or time dependent problems, Runge-Kutta 4th order method is utilized as an efficient technique for solving such problems [41-47]. We applied RK4 method for numerically solving this system, ODE's, where represented mathematically as follow [41-47]:

$$F(x_i,y_j,z_k,t_0+\Delta t)=f(x_i,y_j,z_k,t_0)+\frac{1}{6}\Big[E_1^{ijk}+2E_2^{ijk}+2E_3^{ijk}+E_4^{ijk}\Big],\tag{3.9}$$

where

$$E_1^{ijk}=\Delta t\frac{df}{dt}(u_{ijk},v_{ijk},w_{ijk},p_{ijk},\rho_{ijk},t_0),\tag{3.10a}$$

$$E_2^{ij}=\Delta t\frac{df}{dt}\Big(u_{ijk}+\frac{E_1^{ijk}}{2},v_{ijk}+\frac{E_1^{ijk}}{2},w_{ijk}+\frac{E_1^{ijk}}{2},p_{ijk}+\frac{E_1^{ijk}}{2},\rho_{ijk}+\frac{E_1^{ijk}}{2},t_0+\frac{\Delta t}{2}\Big),\tag{3.10b}$$

$$E_3^{ij}=\Delta t\frac{df}{dt}\Big(u_{ijk}+\frac{E_2^{ijk}}{2},v_{ijk}+\frac{E_2^{ijk}}{2},w_{ijk}+\frac{E_2^{ijk}}{2},p_{ijk}+\frac{E_2^{ijk}}{2},\rho_{ijk}+\frac{E_2^{ijk}}{2},t_0+\frac{\Delta t}{2}\Big),\tag{3.10c}$$

$$E_4^{ij}=\Delta t\frac{df}{dt}\Big(u_{ijk}+E_3^{ijk},v_{ijk}+E_3^{ijk},w_{ijk}+E_3^{ijk},p_{ijk}+E_3^{ijk},\rho_{ijk}+E_3^{ijk},t_0+\Delta t\Big).\tag{3.10d}$$

We will stop if the condition of convergence is achieved as follow [59]:

$$\begin{aligned}&\left|\frac{u_{hx+1}}{u_{hx}}\right|<1,\quad\left|\frac{v_{hx+1}}{v_{hx}}\right|<1,\quad\left|\frac{w_{hx+1}}{w_{hx}}\right|<1,\\&\left|\frac{p_{hx+1}}{p_{hx}}\right|<1,\quad\left|\frac{\rho_{hx+1}}{\rho_{hx}}\right|<1,\quad hx=0,1,2,\cdots.\end{aligned}\tag{3.11}$$

# 4 Numerical results

In this section, some numerical results are presented for the system of unsteady gas flow in (3+1)-dimensional in Eqs. (2.1a)-(2.1e). This system is solved by four quadrature techniques combined with Runge-Kutta 4th order and then a MATLAB code is designed for each method to obtain the numerical results.

To get the reliability, stability, convergence, and efficiency of the numerical results, the present results are compared with the exact ones [8]. Also, various statistical analysis like rate of convergence (ROC), order of convergence $(P)$, Absolute error, RMS, $L_2$ and $L_\infty$ errors are used for the same purpose. The formulas of various statistical analysis are given by [70-71]:

$$\text{Absolute Error}(\varepsilon)=\left|f_{numerical}(x_i,y_j,z_k,t_l)-f_{exact}(x_i,y_j,z_k,t_l)\right|, \tag{4.1a}$$

$$\text{RMS Error}=\sqrt{\left[\sum_{i,j,k=1}^{N_x,N_y,N_z}\left(f_{numerical}(x_i,y_j,z_k,t_l)-f_{exact}(x_i,y_j,z_k,t_l)\right)^2\right]\Big/ N_xN_yN_z}, \tag{4.1b}$$

$$L_2\ \text{Error}=\sqrt{\Delta x\Delta y\Delta z\sum_{i,j,k=1}^{N_x,N_y,N_z}\left(f_{numerical}(x_i,y_j,z_k,t_l)-f_{exact}(x_i,y_j,z_k,t_l)\right)^2}, \tag{4.1c}$$

$$L_\infty\ \text{Error}=\max_{\substack{1\le i\le N_x\\ 1\le j\le N_y\\ 1\le k\le N_z}}\left|f_{numerical}(x_i,y_j,z_k,t_l)-f_{exact}(x_i,y_j,z_k,t_l)\right|, \tag{4.1d}$$

$$\text{Rate of convergence (ROC)}=\log_2\left(\frac{EE^k}{EE^{k-1}}\right), \tag{4.1e}$$

$$\text{Order of convergence}(P)=\log\left(\frac{\varepsilon_{k+1}}{\varepsilon_k}\right)\Big/\log\left(\frac{\varepsilon_k}{\varepsilon_{k-1}}\right), \tag{4.1f}$$

where $k$ is mesh size $(N_x\,X\,N_y\,X\,N_z)$

$$EE=\sqrt{\left[\sum_{i,j,k=1}^{N_x,N_y,N_z}\left(f_{numerical}(x_i,y_j,z_k,t_l)-f_{exact}(x_i,y_j,z_k,t_l)\right)^2\right]\Big/\sum_{i,j,k=1}^{N_x,N_y,N_z}\left(f_{exact}(x_i,y_j,z_k,t_l)\right)^2}.$$

The exact solutions used for comparison are taken from in the literature as follows [8]:

$$u_{(x,y,z,t)}=C_2t-\frac{z}{2}+\frac{C_5-y}{2}+t\ln\left(\frac{z-y}{C_5+2t}\right)-C_1, \tag{4.2a}$$

$$v_{(x,y,z,t)}=\ln\left(\frac{z-y}{C_5+2t}\right)+\frac{y-z}{C_5+2t}+C_2, \tag{4.2b}$$

$$w_{(x,y,z,t)}=\ln\left(\frac{z-y}{C_5+2t}\right)+\frac{y-z}{C_5+2t}+C_2, \tag{4.2c}$$

$$p_{(x,y,z,t)}=C_4(C_5+2t)^{-\gamma},\quad \rho_{(x,y,z,t)}=C_3\frac{(C_5+2t)}{(z-y)^2}, \tag{4.2d}$$

$$0\le t\le T,\quad X_1\le x\le X_2,\quad Y_1\le y\le Y_2,\quad Z_1\le z\le Z_2. \tag{4.2e}$$

## 4.1 Comparison of four DQM results with exact ones

To compare with the available results, the values of $A_i=1$, $B_j=0$, $(i,j=1,2,\cdots,30)$. Table 1 displays the comparison among the non-uniform PDQM, SDQM and exact solution.

Table 1: Numerical solution via Non-uniform PDQM, SDQM and exact solution at $\gamma=1.13$, $y=0.6$, $z=0.5$ and $T=0.111$msec. (For exact solution $C_1=C_2=C_3=C_4=C_5=1$).

| NxxNyxNz | | Exact [8] | Non-uniform DQM | | | SDQM | | |
|---|---|---|---|---|---|---|---|---|
| | | | Computed Results | $L_2$ error | $L_\infty$ error | Computed Results | $L_2$ error | $L_\infty$ error |
| $5\times5\times5$ | $u$ | -1.0501 | -1.0501 | 2.7987e-5 | 3.2532e-7 | -1.0499 | 1.0557e-4 | 1.2922e-6 |
| | $v$ | -1.2028 | -1.2026 | 2.3478e-4 | 2.3484e-6 | -1.2026 | 2.1500e-4 | 1.9072e-6 |
| | $p$ | 0.9997 | 1.0000 | 1.7895e-4 | 2.3357e-6 | 0.9999 | 2.3780e-4 | 3.0441e-6 |
| | $\rho$ | 100.0222 | 100.0065 | 0.0254 | 3.6266e-4 | 100.0013 | 0.0126 | 1.2451e-4 |
| $5\times7\times7$ | $u$ | -1.0501 | -1.0501 | 3.2589e-5 | 6.3011e-7 | -1.0502 | 1.4282e-4 | 3.2888e-6 |
| | $v$ | -1.2028 | -1.2022 | 4.1698e-4 | 9.0320e-6 | -1.2025 | 3.2348e-4 | 6.0042e-6 |
| | $p$ | 0.9997 | 0.9996 | 2.3125e-4 | 5.0454e-6 | 0.9999 | 3.0010e-4 | 7.1013e-6 |
| | $\rho$ | 100.0222 | 99.8533 | 0.1179 | 0.0036 | 99.9949 | 0.0403 | 0.0012 |
| $5\times9\times9$ | $u$ | -1.0501 | -1.0501 | 3.4497e-5 | 9.3029e-7 | -1.0498 | 1.8859e-4 | 6.2035e-6 |
| | $v$ | -1.2028 | -1.2011 | 0.0014 | 7.4531e-5 | -1.2025 | 4.7740e-4 | 1.4737e-5 |
| | $p$ | 0.9997 | 0.9986 | 0.0014 | 3.9588e-5 | 0.9998 | 4.1644e-4 | 1.3668e-5 |
| | $\rho$ | 100.0222 | 98 | 2.5170 | 0.1388 | 100 | 0.3009 | 0.0151 |
| Computation time (sec) | | | 19.307833 at $5\times5\times5$<br>50.407644 at $5\times7\times7$ | | | 17.185643 at $5\times5\times5$<br>45.358427 at $5\times7\times7$ | | |

Table 2: Numerical solution via DSCDQM-DLK, DSCDQM-RSK and exact solution at different bandwidth $(2S+1)$, regularization parameter $\zeta$, and grid size NxxNyxNz ($\gamma=1.13$, $y=1.7$, $z=1.6$ and $T=1.11$msec) (for exact solution $C_1=C_2=C_3=C_4=C_5=1$).

| NxxNyxNz | | S | DSCDQM-DLK | DSCDQM-RSK | | | | | DSCDQM-RSK |
|---|---|---|---|---|---|---|---|---|---|
| | | | | $\zeta=2m_x$ | $\zeta=5m_x$ | $\zeta=7m_x$ | $\zeta=10m_x$ | $\zeta=15m_x$ | |
| $5\times5\times5$ | $u$ | 1 | -2.1521 | -2.1513 | -2.1515 | -2.1515 | -2.1515 | -2.1515 | -2.1514 |
| | | 2 | -2.1509 | -2.1499 | -2.1492 | -2.1491 | -2.1491 | -2.1491 | |
| | $v=w$ | 1 | -1.2042 | -1.2030 | -1.2031 | -1.2031 | -1.2031 | -1.2031 | -1.2050 |
| | | 2 | -1.2033 | -1.2030 | -1.2031 | -1.2031 | -1.2031 | -1.2031 | |
| | $p$ | 1 | 1.0015 | 1.0002 | 1.0002 | 1.0002 | 1.0002 | 1.0002 | 0.9975 |
| | | 2 | 1.0006 | 1.0002 | 1.0002 | 1.0002 | 1.0002 | 1.0002 | |
| | $\rho$ | 1 | 100.2447 | 100.0364 | 100.0404 | 100.0408 | 100.0411 | 100.0412 | 100.2220 |
| | | 2 | 100.0840 | 100.0368 | 100.0412 | 100.0416 | 100.0418 | 100.0420 | |
| Computation | time | 1 | 20.816402 | | | 20.465740 | | | – |
| (sec) | | 2 | 22.219444 | | | 22.246534 | | | – |
| $5\times7\times7$ | $u$ | 1 | -2.1525 | -2.1509 | -2.1510 | -2.1510 | -2.1510 | -2.1510 | -2.1514 |
| | | 2 | -2.1501 | -2.1498 | -2.1493 | -2.1493 | -2.1493 | -2.1492 | |
| | $v=w$ | 1 | -1.2054 | -1.2030 | -1.2031 | -1.2031 | -1.2031 | -1.2031 | -1.2050 |
| | | 2 | -1.2015 | -1.2027 | -1.2026 | -1.2026 | -1.2026 | -1.2026 | |
| | $p$ | 1 | 1.0026 | 1.0000 | 1.0000 | 1.0000 | 1.0000 | 1.0000 | 0.9975 |
| | | 2 | 0.9989 | 0.9999 | 0.9998 | 0.9998 | 0.9998 | 0.9998 | |
| | $\rho$ | 1 | 100.4714 | 100.0351 | 100.0390 | 100.0394 | 100.0396 | 100.0397 | 100.2220 |
| | | 2 | 99.8361 | 100.0103 | 100.0009 | 99.9997 | 99.9991 | 99.9987 | |
| Computation | time | 1 | 54.665468 | | | 48.647755 | | | – |
| (sec) | | 2 | 60.597793 | | | 48.705488 | | | – |

This table show that the results via SDQM is more stable and convergence than non-uniform PDQM. Also, the presented results are good agree with exact solutions at grid size $(5\times5\times5)$. Furthermore, the values of statistical analysis as $L_2$ errors $=2\times10^{-4}$, $L_\infty$ errors $=2\times10^{-6}$ at $(5\times5\times5)$ for SDQ technique it achieved less CPU time $=17.18$ second than the classical DQ scheme. Thus, the scheme based on Cardinal sine is stable and accurate than scheme based on Lagrange interpolation polynomials.

Table 2 compares the results of DSCDQM-DLK, DSCDQM-RSK and exact solution. The calculated results show that DSCDQM-DLK are stable and accurate at mesh size

Table 3: The RMS error and Computation time for all proposed schemes of DQ when $\gamma=1.13$ and grid size $(5\times7\times7)$ (for exact solution [8] $C_1=C_2=C_3=C_4=C_5=1$).

| Time | | Non-uniform PDQM | | SDQM | | DSCDQM-DLK | | DSCDQM-RSK | |
|---|---|---|---|---|---|---|---|---|---|
| | | RMS | Comput time(sec) | RMS | Comput time(sec) | RMS | Comput time(sec) | RMS | Comput time(sec) |
| 5.10e-5 | $u$ | 6.0666e-5 | 21.49375 | 5.6252e-5 | 22.33199 | 5.2629e-5 | 23.18151 | 2.1913e-5 | 22.68310 |
| | $v$ | 1.6458e-4 | | 1.2741e-4 | | 2.6371e-4 | | 1.1030e-4 | |
| | $p$ | 9.1480e-5 | | 1.1819e-4 | | 1.7326e-4 | | 4.8214e-5 | |
| | $\rho$ | 0.0991 | | 0.0159 | | 0.0774 | | 0.0151 | |
| 1.11e-4 | $u$ | 1.3201e-4 | 47.53356 | 1.2241e-4 | 53.34495 | 1.1454e-4 | 52.10686 | 4.7697e-5 | 49.08529 |
| | $v$ | 3.5294e-4 | | 2.7727e-4 | | 5.7339e-4 | | 2.4005e-4 | |
| | $p$ | 1.9906e-4 | | 2.5723e-4 | | 3.7733e-4 | | 1.0491e-4 | |
| | $\rho$ | 0.2157 | | 0.0346 | | 0.1682 | | 0.0328 | |
| 1.499e-4 | $u$ | 1.7824e-4 | 66.26420 | 1.6530e-4 | 73.70444 | 1.5468e-4 | 74.56526 | 6.4416e-5 | 73.27504 |
| | $v$ | 4.7377e-4 | | 3.7441e-4 | | 7.7385e-4 | | 3.2417e-4 | |
| | $p$ | 2.6877e-4 | | 3.4736e-4 | | 5.0977e-4 | | 1.4165e-4 | |
| | $\rho$ | 0.2912 | | 0.0467 | | 0.2269 | | 0.0443 | |
| 2.499e-4 | $u$ | 2.9704e-4 | 135.0072 | 2.7551e-4 | 130.1553 | 2.5786e-4 | 139.6777 | 1.0740e-4 | 130.4887 |
| | $v$ | 7.8201e-4 | | 6.2408e-4 | | 0.0013 | | 5.4039e-4 | |
| | $p$ | 4.4790e-4 | | 5.7905e-4 | | 8.5072e-4 | | 2.3605e-4 | |
| | $\rho$ | 0.4853 | | 0.0778 | | 0.3771 | | 0.0739 | |
| 7.499e-4 | $u$ | 8.8964e-4 | 724.3832 | 8.2581e-4 | 772.8073 | 7.7367e-4 | 714.9515 | 3.2254e-4 | 726.1091 |
| | $v$ | 0.0023 | | 0.0019 | | 0.0038 | | 0.0016 | |
| | $p$ | 0.0013 | | 0.0017 | | 0.0026 | | 7.0687e-4 | |
| | $\rho$ | 1.4538 | | 0.2333 | | 1.1146 | | 0.2217 | |
| 0.00111 | $u$ | 0.0013 | 45.22108 | 0.0012 | 51.85603 | 0.0011 | 52.27803 | 4.7768e-4 | 51.48021 |
| | $v$ | 0.0034 | | 0.0028 | | 0.0056 | | 0.0024 | |
| | $p$ | 0.0020 | | 0.0026 | | 0.0038 | | 0.0010 | |
| | $\rho$ | 2.1491 | | 0.3452 | | 1.6324 | | 0.3281 | |

$(5\times7\times7)$ and $S=2$. But DSCDQM-RSK is stable and accurate at mesh size $(5\times5\times5)$ and $S=1$ and $\xi=5^*m_x$. Also, the two methods are more in agreement with the exact one. As well as, the computation time for DSCDQM-RSK $=20.465740$sec while for DSCDQM-DLK $=60.597793$sec.

In Table 3, RMS error is calculated for four schemes based on different shape functions and combined with RK4 at different times $(0.0051\leq t\leq1.11)$msec. Thus, the results in this table explain that the value of RMS error is least in the DSCDQ-RSK at all time and velocity components, pressure, and density. Also, this method achieved the least computation time. This value of CPU time is different at each time.

As well as, Root mean square error (RMSE) for all proposed techniques is presented in Fig. 1 by different the value of $C_3=0.01$. This figure refers to the value of RMSE for $u\leq10^{-4}$, $v=w\leq3e10^{-3}$, $p\leq2e10^{-4}$ and $\rho\leq10^{-4}$ by using PDQM. Also, via SDQM the value of RMSE for $u\leq1.5e10^{-4}$, $v=w\leq1.6e10^{-3}$, $p\leq4e10^{-4}$ and $\rho\leq2e10^{-4}$. Further, the value of RMSE by using DSCDQM-DLK for $u\leq1.1e10^{-3}$, $v=w\leq5.5e10^{-3}$, $p\leq6e10^{-3}$ and $\rho\leq9e10^{-3}$. But, for the scheme DSCDQ-RSK the value of RMSE for $u\leq8e10^{-5}$, $v=w\leq8e10^{-4}$, $p\leq2.3e10^{-4}$, and $\rho\leq2e10^{-4}$. Thus, from Table 3 and Fig. 1, the least RMSE is achieved via DSCDQ-RSK.

Table 4 displays the comparative stability study between the PDQM and DSCDQ-RSK by computing absolute norm error ($\varepsilon$), root mean square error (RMS), relative norm error $(E)$, rate of convergence, and order of convergence at different grid size. From the obtained results, PDQM is first-order accurate for $u$, fourth-order for $v$, $w$, third-order for $p$ and second-order accurate for $\rho$ at mesh size $(5\times7\times7)$. DSCDQM based on RSK at $2S+1=3$, $\xi=5^*m_x$, mesh size $5\times5\times5$ and computation time $=20.568624$ seconds

Table 4: Stability analysis for Non-uniform PDQM and DSCDQ-RSK when $\gamma=1.13$ at time 0.111msec (for exact solution $C_1=C_2=C_3=C_4=C_5=1$).

| | NxxNyxNz | Non-uniform PDQM | | | | | DSCDQM-RSK | | | | |
|---|---|---|---|---|---|---|---|---|---|---|---|
| | | $\varepsilon$ | EE | ROC | $p$ | RMS | $\varepsilon$ | EE | ROC | $p$ | RMS |
| $u$ | 5×3×3 | 9.3893e-6 | 1.3416e-6 | - | - | 3.1298e-6 | 9.5269e-6 | 2.9180e-5 | — | — | 3.1756e-5 |
| | 5×5×5 | 5.5708e-4 | 4.8113e-5 | 5.1644 | 0.1328 | 1.1142e-4 | 6.7510e-5 | 5.0027e-5 | 0.7777 | 1.0729 | 1.1455e-4 |
| | 5×7×5 | 9.5816e-4 | 7.0050e-5 | 0.5420 | 0.5626 | 1.6196e-4 | 5.5185e-4 | 4.0870e-5 | 0.2917 | 0 | 9.3280e-5 |
| | 5×7×7 | 0.0013 | 7.8432e-5 | 0.1631 | 1.8700 | 1.8105e-4 | 5.5185e-4 | 4.0870e-5 | 0 | Inf | 9.3280e-5 |
| | 5×9×9 | 0.0023 | 1.1179e-4 | 0.5113 | — | 2.5759e-4 | 8.2719e-4 | 4.0534e-5 | 0.0119 | — | 9.1911e-5 |
| $v$ | 5×3×3 | 2.1427e-4 | 3.0616e-5 | — | — | 7.1422e-5 | 2.0417e-4 | 7.4787e-5 | — | — | 8.1390e-5 |
| | 5×5×5 | 0.0011 | 9.5280e-5 | 1.6379 | 0.1021 | 2.2064e-4 | 7.9430e-4 | 1.0305e-4 | 0.4625 | 0.3626 | 1.5886e-4 |
| | 5×7×5 | 0.0013 | 9.2803e-5 | 0.0380 | 1.9480 | 2.1457e-4 | 0.0013 | 9.5826e-5 | 0.1049 | 0 | 2.1866e-4 |
| | 5×7×7 | 0.0018 | 1.1313e-4 | 0.2857 | 4.1734 | 2.6115e-4 | 0.0013 | 9.5826e-5 | 0 | Inf | 2.1871e-4 |
| | 5×9×9 | 0.0070 | 3.3923e-4 | 1.5843 | — | 7.8165e-4 | 0.0026 | 1.2576e-4 | 0.3922 | — | 2.8516e-4 |
| $p$ | 5×3×3 | 2.8580e-4 | 4.0837e-5 | — | — | 9.5266e-5 | 2.4010e-4 | 7.6817e-5 | — | — | 8.1600e-5 |
| | 5×5×5 | 9.0902e-4 | 7.8508e-5 | 0.9430 | 0.1645 | 1.8180e-4 | 9.0659e-4 | 9.0008e-5 | 0.2286 | 0.0738 | 1.8132e-4 |
| | 5×7×5 | 7.5151e-4 | 5.4942e-5 | 0.5149 | 1.5013 | 1.2703e-4 | 0.0010 | 7.7221e-5 | 0.2211 | 0 | 1.7622e-4 |
| | 5×7×7 | 0.0010 | 6.3833e-5 | 0.2164 | 3.9605 | 1.4735e-4 | 0.0010 | 7.7221e-5 | 0 | Inf | 1.7624e-4 |
| | 5×9×9 | 0.0031 | 1.4793e-4 | 1.2125 | — | 3.4087e-4 | 0.0019 | 9.4815e-5 | 0.2961 | — | 2.1499e-4 |
| $\rho$ | 5×3×3 | 0.0176 | 0.0025 | — | — | 0.0059 | 0.0122 | 0.0068 | —- | — | 0.0074 |
| | 5×5×5 | 0.0403 | 0.0035 | 0.4854 | 0.2285 | 0.0081 | 0.0427 | 0.0037 | 0.8780 | 0.1772 | 0.0083 |
| | 5×7×5 | 0.0487 | 0.0036 | 0.0036 | 1.5667 | 0.0082 | 0.0342 | 0.0025 | 0.5656 | 0 | 0.0058 |
| | 5×7×7 | 0.0362 | 0.0022 | 0.7105 | 2.8534 | 0.0052 | 0.0342 | 0.0025 | 0 | Inf | 0.0058 |
| | 5×9×9 | 0.0843 | 0.0407 | 4.2095 | — | 0.9377 | 0.0284 | 0.0014 | 0.8365 | — | 0.0032 |
| Comput time (sec) | | 21.113659 for 5×5×5<br>50.958409 for 5×7×7 | | | | | 20.568624 for 5×5×5<br>49.806566 for 5×7×7 | | | | |

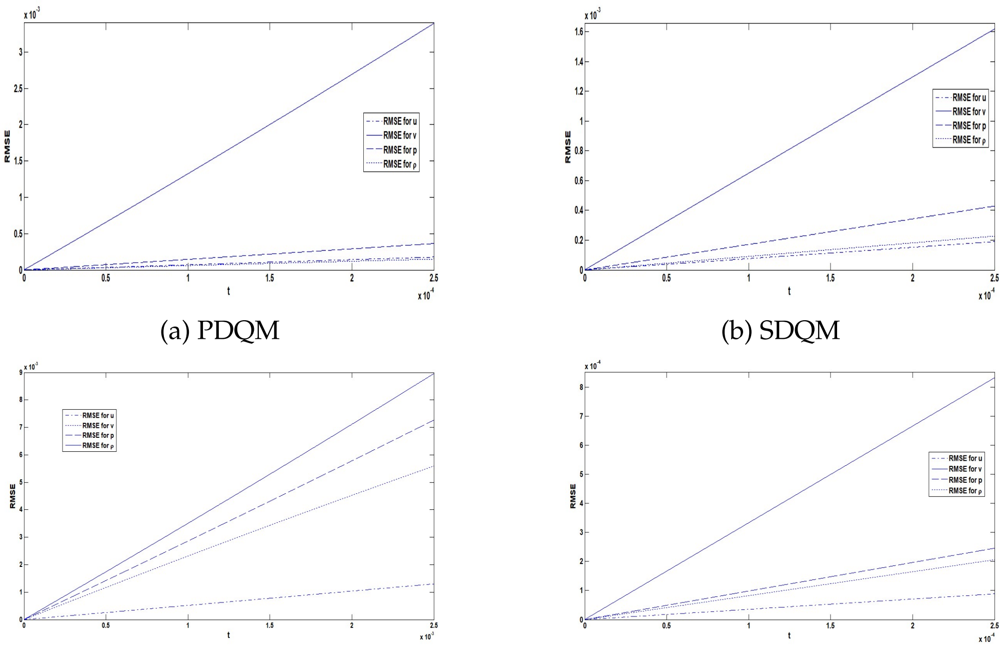


(a) PDQM (b) SDQM

(c) DSCDQM-DLK (d) DSCDQ-RSK

Figure 1: Root mean square error (RMSE) using proposed techniques at $\gamma=1.13$, $C_1=C_2=C_4=C_5=1$ and $C_3=0.01$.

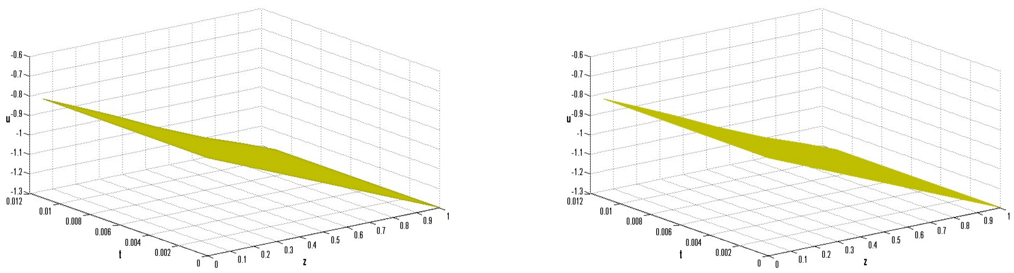

(a) Exact solution (b) DSCDQ-RSK

Figure 2: Velocity component $(u)$ profile at $C_1=C_2=C_5=1$, $y=0.6$ and $\gamma=1.68$ by using Exact solution and DSCDQ-RSK.

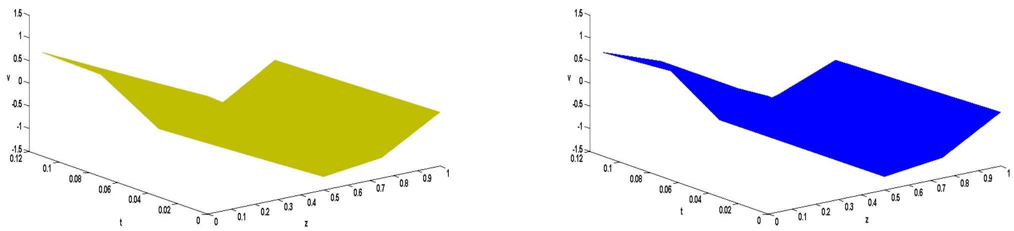

(a) Exact solution (b) DSCDQ-RSK

Figure 3: Velocity component $(v=w)$ profile at $C_1=C_2=C_5=1$, $y=0.6$ and $\gamma=1.68$ by using Exact solution and DSCDQ-RSK.

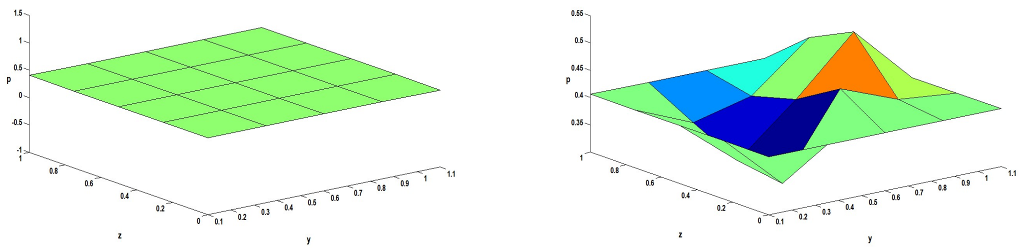

(a) Exact pressure (b) Pressure using DSCDQ-RSK

Figure 4: 3D representations of pressure $(p)$ distribution using Exact solution and DSCDQ-RSK with $C_3=C_4=1$, $C_5=2$ at $t=0.11$sec and $\gamma=1.13$.

gives accurate results better than Classical DQM. Also, the results by DSCDQM-RSK are in a very good agreement with the exact solution $(C_1=C_2=C_3=C_4=C_5=1)$. Further, the order of convergence tends to infinity and the rate of convergence is fast at mesh

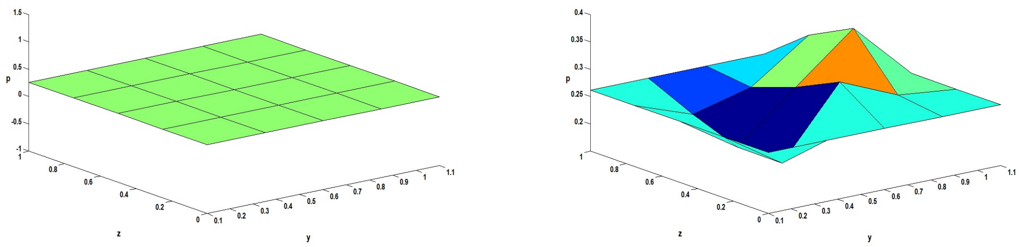

(a) Exact pressure (b) Pressure using DSCDQ-RSK

Figure 5: 3D representations of pressure $(p)$ distribution using Exact solution and DSCDQ-RSK with $C_3=C_4=1$, $C_5=2$ at $t=0.11$sec and $\gamma=1.68$.

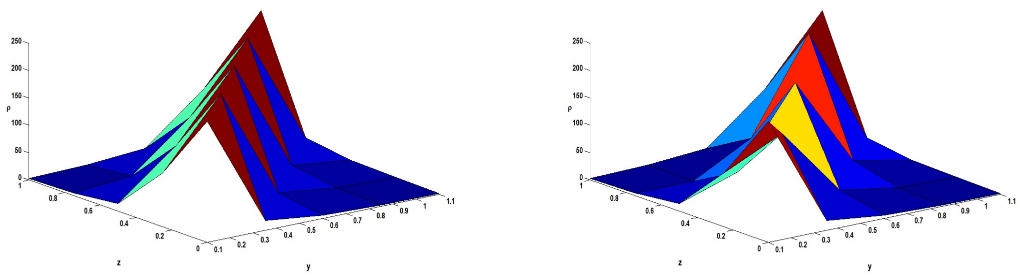

(a) Exact density (b) Density using DSCDQ-RSK

Figure 6: 3D representations of density $(\rho)$ distribution using Exact solution and DSCDQ-RSK with $C_3=C_4=1$, $C_5=2$ at $t=0.11$sec and $\gamma=1.13$.

size $(5\times5\times5)$. From comparison the obtained results by using different schemes, exact solutions, various statistical analysis, and CPU time it is found the method of DSCDQM based on RSK is the better schemes used for solving this system of unsteady gas flow.

Figs. 2-8 show 3-D representations of velocities components profiles $(u,v)$, pressure $(p)$ and density $(\rho)$ via DSCDQM-RSK and Exact solutions at different values of adiabatic index $(\gamma)$ and different locations. In Figs. 2 and 3, it is noticed that velocities components $(u,v=w)$ are agreed with the exact solution at $C_1=C_2=C_5=1$ at $y=0.6$ and $\gamma=1.68$. Also, Figs. 4-7 show the effect of adiabatic index on the pressure $(p)$ and density $(\rho)$ in 3-D distribution by comparing with exact results with $C_3=C_4=1$, $C_5=2$ at $t=0.11$sec. Pressure $(p)$ is affected by change the value of adiabatic index $(\gamma)$ and its value decreases with increasing adiabatic index. Density $(\rho)$ is not influenced by change the value of adiabatic index $(\gamma)$. Further, Figs. 3, 8 display the velocity profile $(v=w)$ influenced by variation the value of $\gamma$ and various locations. Also, these figures show the value of velocity component $(v=w)$ is not approximately affected by change the value of adiabatic index $(\gamma)$.

Fig. 9 displays velocity component $(u)$ where show a linear decrease in the value of

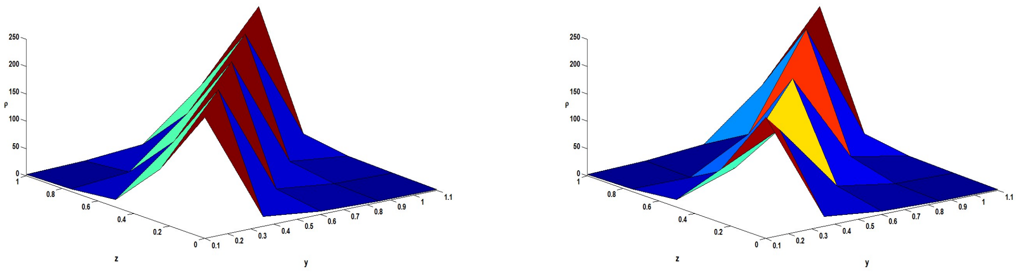

(a) Exact density (b) Density using DSCDQ-RSK

Figure 7: 3D representations of pressure $(p)$ and density $(\rho)$ distribution using Exact solution and DSCDQ-RSK with $C_3 = C_4 = 1$, $C_5 = 2$ at $t = 0.11$sec and $\gamma = 1.68$.

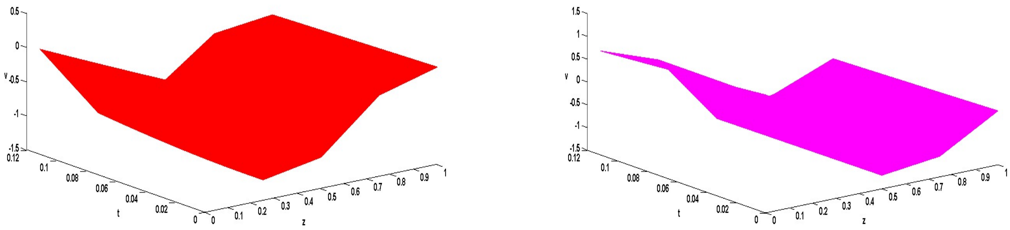

(a) Exact density (b) Density using DSCDQ-RSK

Figure 8: Velocity profile $(v = w)$ using DSCDQ-RSK at $C_2 = C_5 = 1$ and $\gamma = 1.13$.

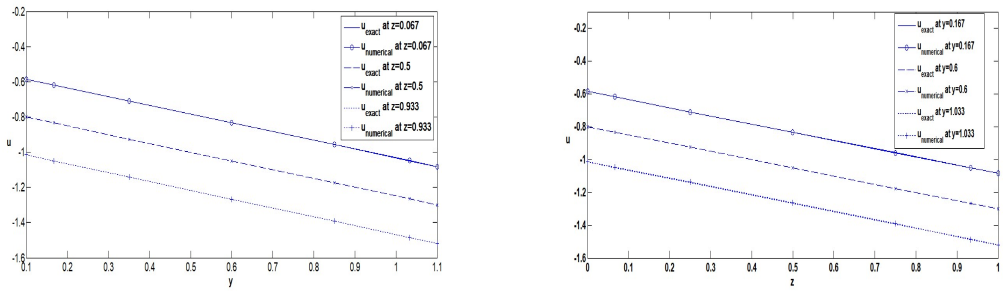

(a) (b)

Figure 9: Velocity component $(u)$ profile using DSCDQM-RSK with $C_1 = C_2 = C_5 = 1$, $t = 1$msec and $\gamma = 1.13$ at different value of $y$, $z$.

velocity at $(0.1 \le y \le 1.1)$, $(0 \le z \le 1.0)$ and $\gamma = 1.13$. Fig. 10 explains velocities components, pressure, and density profiles with time varying in interval $(0 \le t \le 0.012)$ and different locations, showing a velocity in $x$-direction is approximately does not change with time. Also, velocity in $y$-direction decreases with time at $(y = 0.267,\ z = 0.067)$ and $(y = 0.95,$

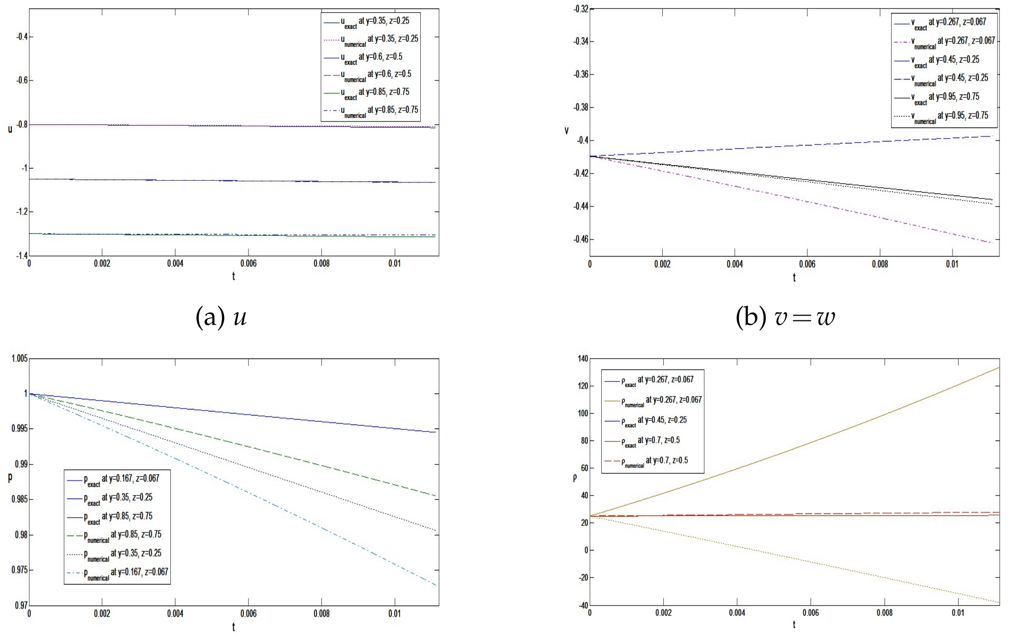

(a) $u$ (b) $v=w$

(c) $p$ (d) $\rho$

Figure 10: Velocities components, pressure and density profiles using DSCDQM-RSK with $C_1=C_2=C_3=C_4=C_5=1$ and $\gamma=1.13$ at different value of $y$, $z$, $t$.

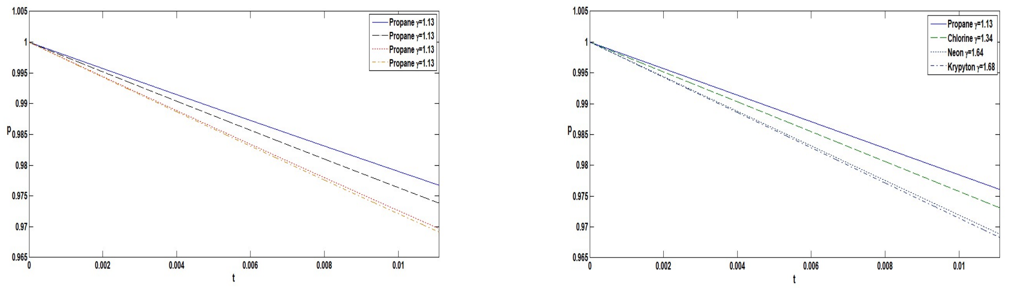


(a) $y=0.6$, $z=0.75$ (b) $y=0.35$, $z=0.5$

Figure 11: Pressure distribution with $C_4=C_5=1$ for different values of adiabatic index $\gamma$ at various materials and locations at 20°C due to DSCDQM-RSK.

$z=0.75$) and increases slightly at ($y=0.45$, $z=0.25$). Pressure is inversely proportional with $t$, $y$, and $z$. The range of pressure is $(0.975 \leq y \leq 1)$ and the initial value is 1 for different locations and it is matching with exact solutions. Further, density decreases with time at ($y=0.45$, $z=0.25$), increases at ($y=0.267$, $z=0.067$) and approximately constant at ($y=0.7$, $z=0.5$).

Figs. 11 and 12 illustrate the influence of $\gamma$ adiabatic index on pressure specially.

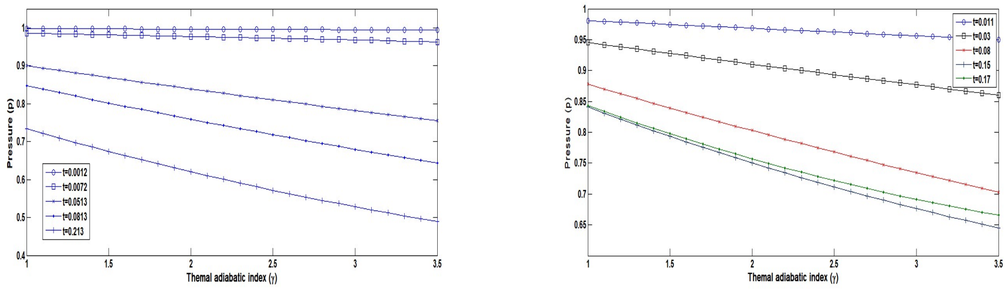


(a) $y=0.35$, $z=0.5$ (b) $y=0.6$, $z=0.75$

Figure 12: The influence of adiabatic thermal index $\gamma$ on the results with $C_4=C_5=1$ due to DSCDQM-RSK at different times and location.

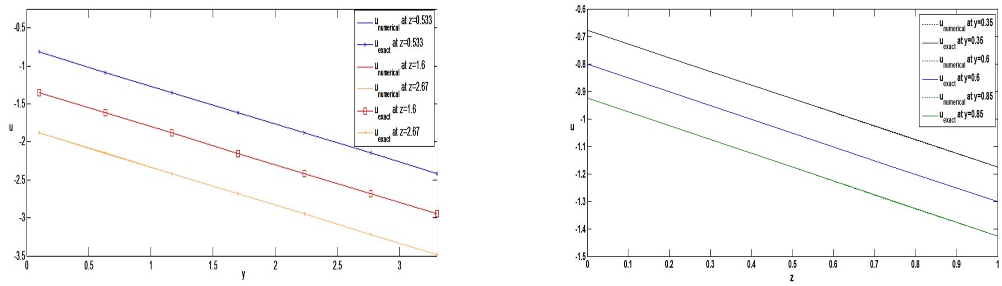


Figure 13: Velocity component $(U)$ profile with $C_1=C_2=C_5=1$ at $t=1.1$msec, different value of $y$, $z$ and $\gamma=1.13$ due to DSCDQM-RSK.

Fig. 11 exhibits that $p$ decreases as $\gamma$ increasing at different materials at 20°C and time $(0\le t\le 0.012)$. Also, Fig. 12 exhibits that pressure $p$ decays during increase time increment and adiabatic index $(\gamma)$. Further, these figures display the $p$ decreasing when $t$ increases. Pressure is approximately does not change with different locations. The relation between pressure and time is closing to linear at little times and the nonlinearity appears at larger times at $t>0.1$sec.

Fig. 13 represents the relation between velocity component $(u)$ with spatial variables $(y$ and $z)$ at $t=1.1$. The exact solution matches very well with the results using DSCDQ-RSK. From this figure, it is shown that $u$ decreases as $y$ and $z$ increase.

## 5 Conclusions

This work investigates four methods based on various shape functions combined with Runge-Kutta 4th order scheme to solve nonlinear four-dimensional unsteady Navier–Stokes equations of gas dynamics. The first one applied polynomial differential quadrature method (PDQM) with Chebyshev discretization. After that, SDQM, DSCDQM-DLK, and DSCDQM-RSK are used. Then, the problem is reduced to system of nonlinear ordinary differential equations. So, Runge-Kutta 4th order (RK4) is employed to complete the solution. A MATLAB program is carried out for solving $(3+1)$-dimensional unsteady gas flow. These methods match very well with the exact results [8]. It is found from the results that PDQM scheme leads to unstable oscillatory results as much as grid size $>11\times11\times11$ and other strategies overcame the instability disadvantages arising with PDQM. But it is found from the comparison with exact solutions and various statistical analysis calculated that the DSCDQM-RSK is more stable, accurate and efficient method with an RMS $\leq10^{-5}$, at mesh size $(5\times5\times5)$, $2S+1=3$, $\xi=5^{*}m_x$ and Computation time $=20.465740$second. Further, the effect of parameter Adiabatic index is examined at different material, different locations and times on the velocities profile, pressure, and density. From the results, it is noticed that the velocities component decreases throughout increasing $y$ and $z$. As well as the value of velocity component $(u,v=w)$ is not affected by change the value of adiabatic index $(\gamma)$. Pressure profile decreases throughout increasing time and adiabatic thermal index. But it approximately does not change with different locations. Also, density increases when increasing the time and is not influenced when the value of adiabatic index $(\gamma)$ changes. On the other hand, we hope to apply these methods for higher dimensional issues in various regions of physical and numerical sciences.

# References


[1] C. SHU AND B. E. RICHARDS, *Application of generalized differential quadrature to solve two-dimensional incompressible Navier-Stokes equations,* Int. J. Numer. Meth. Fluids, 15 (1992), pp. 791–798.

[2] C. SHU AND B. E. RICHARDS, *Parallel simulation of incompressible viscous flows by generalized differential quadrature,* Comput. Syst. Eng., 15 (1992), pp. 271–281.

[3] D. A. ANDERSON, J. C. TANNEHILL AND R. H. PLETCHER, Computational Fluid Mechanics and Heat Transfer, New York: CRC Press, 1984.

[4] I. Y. BABAEV, V. A. BASHKIN AND I. V. EGOROV, *Numerical solution of the Navier–Stokes equations by variational iterative methods,* Zh. Vychisl. Mat. Mat. Fiz., 34 (1994), pp. 1693–1703.

[5] R. M. BEAM AND R. F. WARMING, *An implicit factored scheme for the compressible Navier–Stokes equations,* AIAA J., 16 (1978), pp. 393–402.

[6] T. RAJA SEKHAR AND P. SATAPATHY, *Group classification for isothermal drift flux model of two-phase flows,* Comput. Math. Appl., 72 (2016), pp. 1436–1443.

[7] T. RAJA SEKHAR AND V. D. SHARMA, *Similarity solutions for three dimensional Euler equations using Lie group analysis,* Appl. Math. Comput., 196 (2008), pp. 147–157.

[8] A. S. RASHED, *Analysis of $(3+1)$-dimensional unsteady gas flow using optimal system of Lie symmetries,* Math Comput. Simulat., 156 (2019), pp. 327–346.

[9] J. C FUCHS AND E. W. RICHTER, *Similarity solutions for the two-dimensional non-stationary ideal MHD equations,* J. Phys. A, 20 (1987), pp. 3135–3157.

[10] S. MURATA, *New class of symmetries and exact solution to the unsteady equations of adiabatic gas dynamics,* Chaos Solitons Fract., 24 (2005), pp. 579–582.

[11] R. ARORA, M. J. SIDDIQUI AND V. P. SINGH, *Similarity method for imploding strong shocks in a non-ideal relaxing gas,* Int. J. Nonlinear Mech., 57 (2013), pp. 1–9.

[12] F. OLIVERI AND M. P. SPECIALE, *On the equations of ideal-gas dynamics with a separable equation of state: Lie group analysis and substitution principles,* Int. J. Nonlinear Mech., 27 (1992), pp. 773–784.

[13] F. OLIVERI AND M. P. SPECIALE, *Exact solutions to the equations of ideal gas-dynamics by means of the substitution principle,* Int. J. Nonlinear Mech., 33 (1998), pp. 585–592.

[14] F. OLIVERI AND M. P. SPECIALE, *Exact solutions to the unsteady equations of perfect gases through Lie group analysis and substitution principles,* Int. J. Nonlinear Mech., 37 (2002), pp. 257–274.

[15] F. OLIVERI AND M. P. SPECIALE, *Exact solutions to the equations of ideal gas–dynamics by means of the substitution principle,* Int. J. Nonlinear Mech., 33 (1998), pp. 585–592.

[16] F. OLIVERI AND M. P. SPECIALE, *Exact solutions to the equations of perfect gases through Lie group analysis and substitution principles,* Int. J. Nonlinear Mech., 34 (1999), pp. 1077–1087.

[17] F. OLIVERI AND M. P. SPECIALE, *Exact solutions to the unsteady equations of perfect gases through Lie group analysis and substitution principles,* Int. J. Nonlinear Mech., 37 (2002), pp. 257–274.

[18] F. OLIVERI AND M. P. SPECIALE, *Exact solutions to the ideal magneto–gas–dynamics equations through Lie group analysis and substitution principles,* J. Phys. A Math. Gen., 38 (2005), pp. 8803–8820.

[19] Y. A. CHIRKUNOV, *The conservation laws and group properties of the equations of gas dynamics with zero velocity of sound,* J. Appl. Math. Mech., 73 (2009), pp. 421–425.

[20] I. U. BABAEV, V. A. BASHKIN AND I. V. EGOROV, *Numerical solution of the Navier-Stokes equations using iterative methods of variational type,* Zh. Vych. Matem. Mat. Phys. 34 (1994), pp. 1693–1703.

[21] I. U. BRAILOVSKAYA, *Finite-difference Scheme for the numerical solution of the two-dimensional time-dependent compressible Navier–Stokes equations,* Dokl. Akad. Nauk. SSSR, 160 (1965), pp. 1042–1045.

[22] A. M. BUBENCHIKOV AND D. K. FIRSOV, *Finite-difference scheme for the numerical integration of the compressible Navier–Stokes equations on nonstaggered nonorthogonal grid,* Vest. Tomsk. Univ., 4 (2001), pp. 5–22.

[23] S. K. GODUNOV AND V. S. RYABEN'KII, The Theory of Difference Schemes: An Introduction, North-Holland, 1964.

[24] X. ZHAO, Y. CHEN, L. YANG, N. LIU AND S. SHU, *Efficient boundary condition-enforced immersed boundary method for incompressible flows with moving boundaries,* J. Comput. Phys., 441 (2021), 110425.

[25] Z. YUAN, L. YANG, C. SHU, Z. LIU AND W. LIU, *A novel gas kinetic flux solver for simulation of continuum and slip flows,* Int. J. Numer. Meth. Fluids, 93 (2021), pp. 2863–2888.

[26] Danish Hydraulic Institute, MIKE11 Reference Manual, Denmark, 2003.

[27] US Army Corps of Engineers, HEC-RAS Reference Manual, 2004.

[28] D. ZHOU, Z. LU, T. GUO AND L. YANG, *Development of circular function-based gas-kinetic scheme (CGKS) on moving grids for unsteady flows through oscillating cascades,* Int. J. Numer. Meth. Fluids, 84 (2017), pp. 715–736.

[29] L. YANG, C. SHU, Z. CHEN, Y. WANG AND G. HOU, *A simplified lattice Boltzmann flux solver for multiphase flows with large density ratio,* Int. J. Numer. Meth. Fluids, 93 (2021), pp. 1895–1912.

[30] K. S. SHTEREV, *Iterative process acceleration of calculation of unsteady, viscous, compressible, and*

*heat-conductive gas flows,* Int. J. Numer. Meth. Fluids, 77 (2015), pp. 108–122.

[31] C. LAI, *Numerical modeling of unsteady open-channel flow,* in Advances in Hydroscience, edited by V. T. Chow, Academic Press, 1986, pp. 162–323.

[32] C. SHU, B. C. KHOO AND K. S. YEO, *Numerical solution of incompressible Navier–Stokes equations by generalized differential quadrature,* Finite Elem. Anal. Des., 18 (1994), pp. 83–97.

[33] C. SHU, B. C. KHOO AND K. S. YEO, *Application of GDQ scheme to simulate incompressible viscous flows around complex geometries,* Mech. Res. Commun., 22 (1994), pp. 319–325.

[34] C. SHU, B. C. KHOO, Y. T. CHEW AND K. S. YEO, *Solutions of three-dimensional boundary layer equations by global methods of generalized differential–integral quadrature,* Comput. Meth. Appl. Mech. Eng., 135 (1996), pp. 229–241.

[35] C. SHU, Differential Quadrature and Its Application in Engineering, Springer-Verlag, 2000.

[36] J. SUN AND Z. Y. ZHU, *Upwind local differential quadrature method for solving incompressible viscous flow,* Comput. Meth. Appl. Mech. Eng., 188 (2000), pp. 495–504.

[37] C. SHU, L. WANG AND Y. T. CHEW, *Numerical computation of three-dimensional incompressible Navier–Stokes equations in primitive variable form by DQ method,* Int. J. Numer. Meth. Fluids, 43 (2004), pp. 345–368.

[38] M. A. DE ROSA, M. A. LIPPIELLO, AND R. JIWARI, *A differential quadrature based procedure for parameter identification,* Appl. Math. Comput., 290 (2016), pp. 460–466.

[39] A. M. ALQAHTANI AND R. JIWARI, *Wavelet operational matrices and Lagrange interpolation differential quadrature-based numerical algorithms for simulation of nanofluid in porous channel,* J. Math., (2022).

[40] R. H. MOHAMMAD, J. A. MOHAMMAD AND M. PARVIZ, *A differential quadrature analysis of unsteady open channel flow,* Appl. Math. Model., 31 (2007), pp. 1594–1608.

[41] P. BIRKEN, *Optimizing Runge-Kutta smoothers for unsteady flow problems,* Electron. Trans. Numer. Anal., 39 (2012), pp. 298–312.

[42] A. JAMESON, *Evaluation of fully implicit Runge Kutta schemes for unsteady flow calculations,* J. Sci. Comput., (2017).

[43] T. Y. SHENG, *Runge-Kutta methods combined with compact difference schemes for the unsteady Euler equations,* Center Model Turbulence Transition, (1991), pp. 127–199.

[44] H. YUAN AND C. SONG, *Nonlinear stability and convergence of two-step Runge-Kutta methods for Volterra delay integro-differential equations,* Abstr. Appl. Anal., (2013), pp. 1–13.

[45] M. SALAH, R. M. AMER AND M. S. MATBULY, *Analysis of reaction diffusion problems ssing differential quadrature method,* Int. J. Eng. Tech., 13 (2013).

[46] M. SALAH, R. M. AMER AND M. S. MATBULY, *An efficient method to solve thermal wave equations,* Appl. Math., 5 (2014), pp. 542–552.

[47] M. SALAH, R. M AMER AND M. S. MATBULY, *The differential quadrature solution of reaction-diffusion equation using explicit and implicit numerical schemes,* Appl. Math., 5 (2014), pp. 327–336.

[48] A. H. MSMALI, M. TAMSIR, AND A. A. AHMADINI, *Crank-Nicolson-DQM based on cubic exponential B-splines for the approximation of nonlinear Sine-Gordon equation,* Ain Shams Eng. J., 12 (2021), pp. 4091–4097.

[49] M. TAMSIR, N. DHIMAN, AND F. S. GILL ROBIN, *Approximation of 3D convection diffusion equation using DQM based on modified cubic trigonometric B-splines,* J. Comput. Methods Sci. Eng., 20 (2020), pp. 1357–1366.

[50] M. TAMSIR AND N. DHIMAN, *DQM based on the modified form of CTB shape functions for coupled Burgers' equation in 2D and 3D,* Int. J. Math. Eng. Manag. Sci., 4 (2019), pp. 1051–1067.

[51] M. TAMSIR, *Cubic trigonometric B-spline differential quadrature method for numerical treatment*

*of Fisher's reaction-diffusion equations,* Alex. Eng. J., 53 (2018), pp. 2019–2026.

[52] M. TAMSIR, V. K. SRIVASTAVA, N. DHIMAN, AND A. CHAUHAN, *Numerical computation of nonlinear Fisher's reaction–diffusion equation with exponential modified cubic B-spline differential quadrature method,* Int. J. Appl. Comput. Math., 6 (2018), 4.

[53] M. TAMSIR, V. K. SRIVASTAVA, AND R. JIWARI, *An algorithm based on exponential modified cubic B-spline differential quadrature method for nonlinear Burgers' equation,* Appl. Math. Comput., 290 (2016), pp. 111–124.

[54] H. SHUKLA, M. TAMSIR, R. JIWARI, AND V. SRIVASTAVA, *A numerical algorithm for computation modeling of 3D nonlinear wave equations based on exponential modified cubic B-spline differential quadrature method,* Int. J. Comput. Math., 95 (2018), pp. 752–766.

[55] H. SHUKLA, M. TAMSIR, V. SRIVASTAVA, AND M. RASHIDI, *Modified cubic B-spline differential quadrature method for numerical solution of three-dimensional coupled viscous Burger equation,* Modern Phys. Lett. B, 30 (2016).

[56] H. S. SHUKLA, M. TAMSIR, AND V. K. SRIVASTAVA, *Numerical simulation of two dimensional sine-Gordon solitons using modified cubic B-spline differential quadrature method,* AIP Adv., 5 (2015).

[57] M. EL-GAMEL AND A. ZAYED, *A comparison between the wavelet Galerkin and the sinc Galerkin methods in solving nonhomogeneous heat equations,* in Inverse Problems, Image Analysis, and Medical Imaging, 2002, edited by N. Zuhair AND S. Otmar, 313, AMS, Providence, 2002.

[58] G. YIN, *Sinc-collocation method with orthogonalization for singular problem-like poisson,* Math. Comput., 62 (1994), pp. 21–40.

[59] T. S. CARLSON, J. DOCKERY AND J. LUND, *A sinc-collocation method for initial value problems,* Math. Comput., 66 (1997), pp. 215–235.

[60] C. H. W. NG, Y. B. ZHAO AND G. W. WEI, *Comparison of discrete singular convolution and generalized differential quadrature for the vibration analysis of rectangular plates,* Comput. Meth. Appl. Mech. Eng., 193 (2004), pp. 2483–2506.

[61] G. W. WEI, *Discrete singular convolution for the Fokker–Planck equation,* Chem. Phys., 110 (1999), pp. 8930–8942.

[62] G. W. WEI, *A unified method for solving Maxwell's equation,* in Preceding of Asia Pacific Microwave Conference, Singapore, 1999, pp. 562–565.

[63] G. W. WEI, *Solving quantum eigenvalue problems by discrete singular convolution,* J. Phys. B, 33 (2000), pp. 343–352.

[64] G. W. WEI, *A unified approach for solving the Fokker–Planck equation*, J. Phys. A, 33 (2000), pp. 4935–4953.

[65] G. W. WEI, Y. B. ZHAO AND Y. XIANG, *A novel approach for the analysis of high frequency vibrations,* J. Sound. Vib., 257 (2002), pp. 207–246.

[66] G. W. WEI, *A new approach for solving some mechanical problems,* Comput. Methods. Appl. Mech. Eng., 190 (2001), pp. 2017–2030.

[67] D. C. WAN AND G. W. WEI, *Discrete singular convolution-finite subdomain method for the solution of incompressible viscous flows,* J. Comput. Phys., 180 (2002), pp. 229–255.

[68] G. W. WEI, Y. B. ZHAO AND Y. XIANG, *The determination of natural frequencies of rectangular plates with mixed boundary conditions by discrete singular convolution,* Int. J. Mech. Sci., 43 (2001), pp. 1731–1746.

[69] G. W. WEI, *Discrete singular convolution for the solution of the Fokker-Planck equations,* J. Chem. Phys., 110 (1999), pp. 8930–8942.

[70] N. HILAL, S. INJROU AND R. KARROUM, *Exponential finite difference methods for solving Newell–Whitehead–Segel equation,* Arab. J. Math., 9 (2020), pp. 367–379.

[71] R. JIWARI. K. GUPTA AND V. KUMAR, *Polynomial differential quadrature method for numerical solutions of the generalized Fitzhugh-Nagumo equation with time-dependent coefficients,* Ain Shams Eng. J., 5 (2014), pp. 1343–1350.